environmental microbiology

Environmental Microbiology (2021) **23**(10), 5823–5836 doi:10.1111/1462-2920.15513

Special Issue Article

D-canavanine affects peptidoglycan structure, morphogenesis and fitness in Rhizobiales

Alena Aliashkevich,[1] Matthew Howell,[2,3] Pamela J. B. Brown[2] and Felipe Cava[1]*

[1]*Department of Molecular Biology and Laboratory for Molecular Infection Medicine Sweden, Umeå Centre for Microbial Research, Umeå University, Umeå, Sweden.*

[2]*Division of Biological Sciences, University of Missouri, Columbia, MO, 65201.*

[3]*Department of Biology and Environmental Science, Westminster College, Fulton, MO, 65251.*

Summary

The bacterial cell wall is made of peptidoglycan (PG), a polymer that is essential for maintenance of cell shape and survival. Many bacteria alter their PG chemistry as a strategy to adapt their cell wall to external challenges. Therefore, identifying these environmental cues is important to better understand the interplay between microbes and their habitat. Here, we used the soil bacterium *Pseudomonas putida* to uncover cell wall modulators from plant extracts and found canavanine (CAN), a non-proteinogenic amino acid. We demonstrated that cell wall chemical editing by CAN is licensed by *P. putida* BSAR, a broad-spectrum racemase which catalyses production of DL-CAN from L-CAN, which is produced by many legumes. Importantly, D-CAN diffuses to the extracellular milieu thereby having a potential impact on other organisms inhabiting the same niche. Our results show that D-CAN alters dramatically the PG structure of Rhizobiales (e.g., *Agrobacterium tumefaciens*, *Sinorhizobium meliloti*), impairing PG crosslinkage and cell division. Using *A. tumefaciens*, we demonstrated that the detrimental effect of D-CAN is suppressed by a single amino acid substitution in the cell division PG transpeptidase penicillin binding protein 3a. Collectively, this work highlights the role of amino acid racemization in cell wall chemical editing and fitness.

Received 28 January, 2021; revised 25 March, 2021; accepted 6 April, 2021. *For correspondence. +46-90 785 6755; E-mail felipe.cava@umu.se

Introduction

Bacteria establish a myriad of complex social structures with other living organisms in the biosphere that frequently involve competitive and cooperative behaviours (Keller and Surette, 2006; Duran *et al*., 2018). For instance, many mutualists rely on each other for nutrients and protection (Mandel *et al*., 2009; Poliakov *et al*., 2011; Kim *et al*., 2019). Evolution has consolidated these partnerships by selecting specific mechanisms that provide a mutual benefit to the partners, making the interactions more efficient and robust. A representative example of mutualism is the case of legume plants and rhizobia bacteria. Legumes produce flavonoid signals to recruit nitrogen fixing bacteria to the plant. Microbes provide nitrogen in return for energy-containing carbohydrates (Djordjevic *et al*., 1987; Long, 1989; Shaw *et al*., 2006). Nowadays, it is considered that these types of plant–bacteria interactions are more widespread in nature than was previously thought (Doebeli and Knowlton, 1998; Berendsen *et al*., 2018).

The development of specific social relationships often requires communication strategies. One such strategy is the production and release of small diffusible molecules, which facilitate interactions between organisms in the distance and often are instrumental to shape the biodiversity, dynamics and ultimately, the biological functions of the ecosystems (Scott *et al*., 2008). Many taxonomically unrelated bacteria produce non-canonical D-amino acids (NCDAAs) to the extracellular milieu in order to regulate diverse cellular processes at a population level. The regulatory properties of NCDAA seem to be specific for each D-AA, e.g., D-Met and D-Leu downregulate peptidoglycan(PG) synthesis (Lam *et al*., 2009; Cava *et al*., 2011; Hernandez *et al*., 2020), D-Ala represses spore germination (Hills, 1949) and D-Arg affects phosphate uptake (Alvarez *et al*., 2018; reviewed in Aliashkevich *et al*., 2018).

The modulatory effects of NCDAA on the cell wall require that these molecules replace the canonical D-Alanine located at the terminal position (fourth or fifth) of

the PG peptide stems. NCDAA editing at fourth position is catalysed by LD-transpeptidases (Ldts), which are enzymes involved in PG crosslinking (i.e., dimer synthesis) through the formation of meso-diaminopimelic acid (mDAP-mDAP) peptide bridges (Cava *et al*., 2011). In contrast, incorporation of NCDAA at the fifth position is mediated by penicillin binding proteins (PBPs) with DD-transpeptidase activity (Kuru *et al*., 2019) or by synthesis of modified precursors in the cytoplasmic *de novo* synthetic pathway (Cava *et al*., 2011). These changes in muropeptides composition induced by NCDAA can have an obvious impact on many enzymes, which synthesize and remodel the PG.

Production of many NCDAAs depends on the enzyme broad-spectrum racemase (Bsr), which converts L-amino acids, protein building blocks, into D-AAs (Espaillat *et al*., 2014). In *Vibrio cholerae*, BsrV is located in the periplasmic space (Lam *et al*., 2009), which is consistent with the prediction of a signal peptide in most Bsr homologues (Espaillat *et al*., 2014). Distribution of Bsr-bacteria across diverse ecological niches (Espaillat *et al*., 2014) together with the metabolic investment in producing NCDAA suggests an important physiological role for these molecules. It is worth mentioning that the capacity to incorporate NCDAA in the PG is widespread in bacteria. The fact that non-Bsr organisms can be also influenced by PG editing suggests that NCDAA can act as engines of biodiversification within poly-microbial communities (Alvarez *et al*., 2018).

Although the implications of NCDAAs in microbial ecology are rapidly growing, yet most studies focus on the production of D-AAs from their proteinogenic L-counterparts while non-proteinogenic amino acids are much less studied. Here, we report that broad spectrum amino acid racemase of the soil bacterium *Pseudomonas putida* (BSAR) can effectively produce DL-canavanine (DL-CAN) from L-CAN, an allelopathic non-proteinogenic amino acid produced by many agronomically important legumes (e.g., alfalfa, jack beans) in high amounts (Bell, 1958; Rosenthal and Nkomo, 2000). L-CAN is located primarily in seeds and serves not only as protection against herbivores, but also as nitrogen storage, and reaches 5% of the total seed dry matter in *Canavalia ensiformis* (jack bean) and even exceeds 10% of the total seed dry matter in *Dioclea megacarpa* (Rosenthal, 1970, 1977).

Previous studies have reported that L-CAN inhibits growth of plants that do not produce L-CAN (e.g., tomato, cabbage) due to the induction of systemic protein misfolding associated with the capacity of L-CAN to replace L-Arginine in proteins (Rosenthal and Dahlman, 1991; Miersch *et al*., 1992).

Since D-CAN diffuses from *P. putida* to the extracellular media, we hypothesized that this D-AA might impact the fitness and/or physiology of nearby bacteria in line with previous studies that highlight the role of interspecies competition in modulating the plant microbiome (Hibbing *et al*., 2010; Bakker *et al*., 2014). Our results suggest that while DL-CAN is less toxic to *Arabidopsis thaliana* growth, the former is more inhibitory to certain rhizosphere-associated bacteria. Further mechanistic investigation revealed that D-CAN is incorporated in high amounts in the cell wall of Rhizobiales species. Cell wall chemical editing by DL-CAN affects PG structure which causes cell division impairment and fitness loss. Using the plant pathogen *Agrobacterium tumefaciens*, we demonstrated that DL-CAN deleterious effects on cell wall integrity can be alleviated by just a single amino acid substitution in the cell division PG transpeptidase penicillin binding protein 3a (PBP3a).

Results

Bacterial racemization of CAN licences its incorporation into the cell wall

To identify new environmental modulators of the bacterial cell wall, we tested the capacity of alfalfa (*Medicago sativa*) seed extract to induce changes in the PG chemical structure of *Pseudomonas putida* – a bacterium, which is an efficient root and rhizosphere colonizer with a wide catabolic potential and plant growth-promoting properties (Weller, 1988; Molina *et al*., 2000; Fig. 1A). We found that *P. putida* PG profile displayed a new potential muropeptide (peak 3) when supplemented with the extract (Fig. 1B). By mass spectrometry, we identified that peak 3 corresponded to a disaccharide tetrapeptide where the C-terminal D-Alanine was replaced by a molecule with monoisotopic mass of 176.115 mass units (u) (Fig. S1, Fig. S2A and B). *In silico* search using the biologic magnetic resonance data bank (https://bmrb.io/metabolomics/mass_query.php) for compounds with similar masses to the one identified (± 0.025 u) and preferably containing amino groups pointed L-CAN as the most likely candidate, as this is a non-proteinogenic amino acid produced by legumes. Consistently, PG analysis of *P. putida* cultures supplemented with pure L-CAN showed a peak with similar retention time and MS fragmentation profile as peak 3 (Fig. 1C, Fig. S2C and D), which further co-eluted when the first was purified and spiked in the PG sample of *P. putida* grown with alfalfa seed extract (Fig. S2E). Therefore, we renamed peak 3 as $M4^{CAN}$. Additionally, PG of *P. putida* cultures grown with L-CAN also displayed a dimeric muropeptide containing CAN in fourth position of the peptide moiety ($D44^{CAN}$) (Fig. 1C, Fig. S2C and F).

Since the fourth position in the peptide moiety of muropeptides is normally restricted to D-AAs, we hypothesized that *P. putida* might have produced DL-CAN from

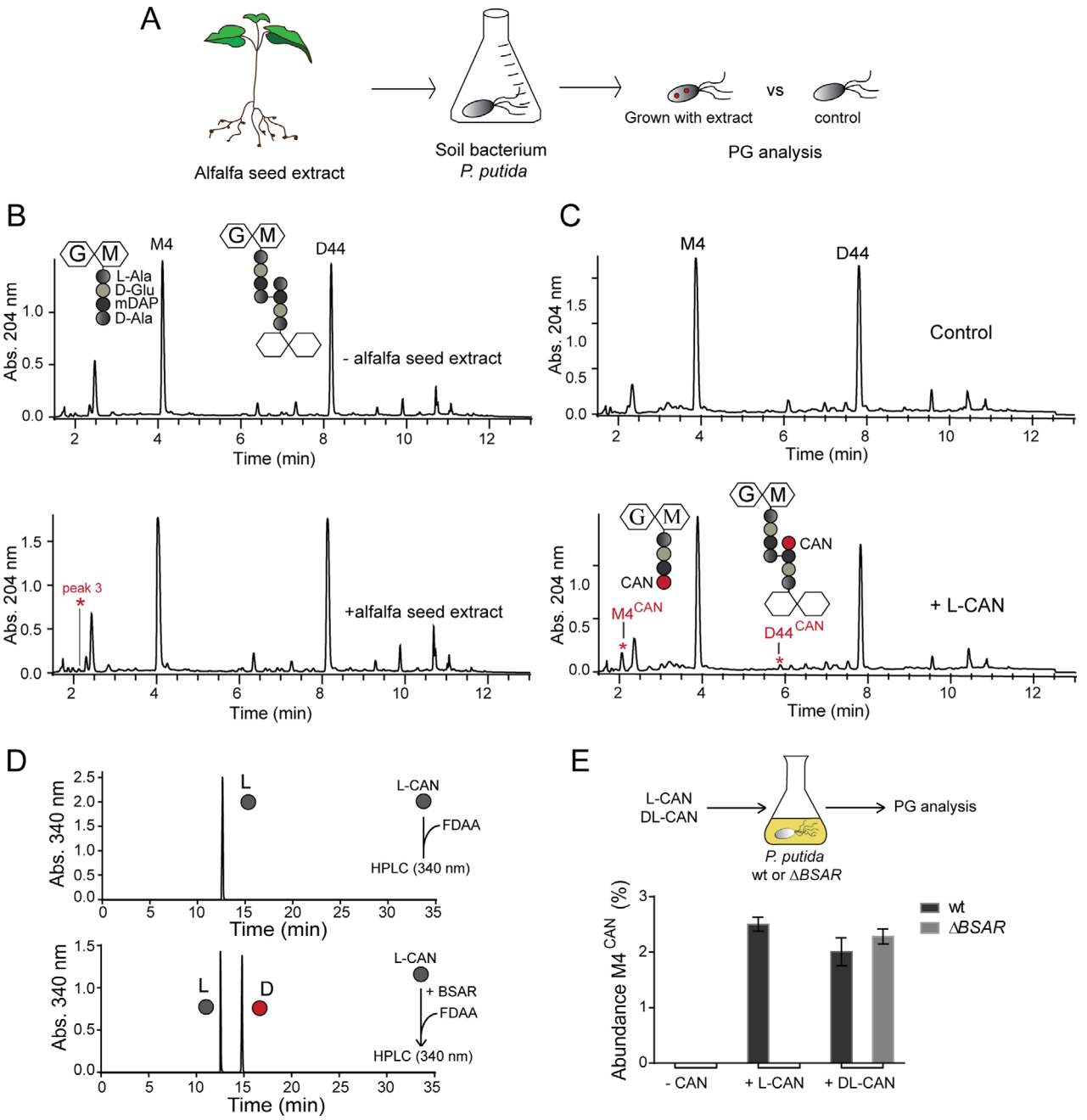

Fig 1. DL-CAN is produced from L-CAN.
A. Scheme of PG-modifying metabolites identification.
B. Modified M4 was found in the sample grown with *Medicago sativa* (alfalfa) seeds extract.
C. Cell wall analysis of *Pseudomonas putida*, grown without (control) or with addition of L-CAN 5 mM.
D. HPLC analysis of Marfey's derivatized L-CAN and L-CAN incubated with *P. putida* broad-spectrum racemase BSAR.
E. Cell wall analysis of *P. putida* wt and Δ*BSAR* mutant, grown in the presence of L- or DL-CAN 5 mM or without.

L-CAN. In fact, *P. putida* genome encodes a periplasmic broad-spectrum amino acid racemase (PP3722; renamed from alanine racemase Alr to BSAR by Radkov and Moe) (Radkov and Moe, 2013, 2018). To test whether PP3722 could racemize CAN, we purified the protein and performed *in vitro* racemization assays using pure L-CAN as substrate. Indeed, using High Performance Liquid Chromatography (HPLC), we observed that BSAR converted L-CAN into a mixture of DL-CAN (Fig. 1D). Consistently, deletion of *BSAR* in *P. putida* produced a strain incapable to make D-CAN-containing muropeptides in L-CAN supplemented cultures (Figs. S3A and S3B). PG edited with CAN was produced by *P. putida* Δ*BSAR* only when exogenously supplemented with DL-CAN (Fig. 1E).

Since we did not succeed in purifying D-CAN, we used DL-CAN racemic mixture as a source of D-CAN (DL-CAN). In addition, supplementation of wild-type *P. putida* with diverse L-AAs (Ala, Leu, Ser, Met, Arg and CAN) resulted in measurable levels of D-AAs in supernatant. Conversely, no D-AAs were detected in BSAR deficient strain, except for low levels of D-Ala, which likely resulted from the Alanine racemase activity (Fig. S3C).

In agreement with these results, DL-CAN containing supernatants (from wild-type (wt) *P. putida*) induced production of D-CAN muropeptides in *Escherichia coli*, a bacterium that lacks broad-spectrum racemase (Fig. S3D), indicating that D-CAN diffuses to the environment most likely through outer membrane porins from *P. putida* cells and can modify PG of other bacteria. As expected, no D-CAN muropeptides were induced in *E. coli* when this bacterium was cultured with preconditioned media from the Δ*BSAR* strain. Collectively, these results indicate that bacterial broad-spectrum racemase BSAR can change the chirality of plant-derived amino acid L-CAN, thereby licensing its D-form for PG editing.

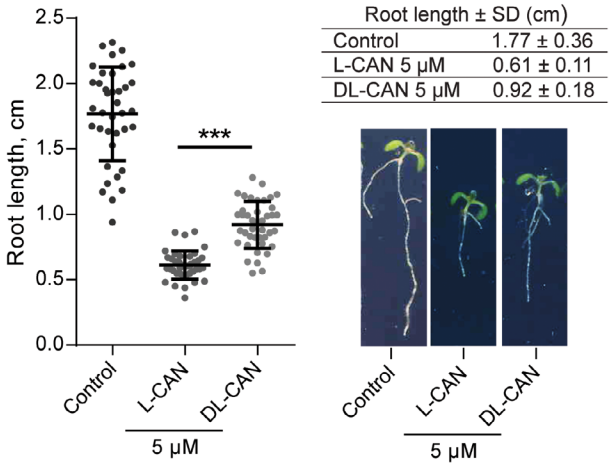

Fig 2. Functionality of D-CAN is different from L-CAN. Root length in *Arabidopsis thaliana* grown on ½ Murashige–Skoog agar supplemented with L- or DL-CAN 5 μM or not (control). Pictures show representative plants. *P* value <0.0001 (***).

Enantiomerization changes the functionality of CAN

Previous studies showed that production of L-CAN by legumes underlies a defensive strategy against certain competitors (e.g., plants, insects; Dahlman and Rosenthal, 1975, 1976; Miersch *et al*., 1992) based on the incorporation of this toxic atypical amino acid into proteins due to its chemical similarities with L-arginine (Pines *et al*., 1982; Rosenthal *et al*., 1989; Rosenthal and Dahlman, 1991). Compared to L-CAN, there is virtually no information about D-CAN. Thus, to understand the biological role of this D-AAs, we first checked if DL-CAN displayed the same activity as L-CAN. In agreement with previous reports, L-CAN inhibited root growth of *A. thaliana* seedlings at 5 μM concentration with the resulting root length almost three times shorter than in control (Fig. 2). However, the average root length in the presence of DL-CAN 5 μM was 1.5 times longer than that grown with the same concentration of L-CAN suggesting that CAN enantiomers have different functions. Indeed, additional experiments comparing root lengths at L-CAN 5 μM versus DL-CAN 10 μM (i.e., 5 μM D-CAN + 5 μM L-CAN), and L-CAN 10 μM versus DL-CAN 20 μM (i.e., 10 μM D-CAN + 10 μM L-CAN), where in both cases molar ratio of L-form is the same, revealed no significant differences between them (Fig. S4A) and suggests that only L-CAN inhibits root development in *A. thaliana*. Interestingly, in addition to tap root length, development of lateral roots and root hairs were also affected by L-CAN, but not by D-CAN (Fig. S4B). Collectively, these results stress the idea that CAN enantiomers have different activities.

DL-CAN severely alters cell wall composition in Rhizobiales

To ascertain the physiological role of DL-CAN, we investigated its effect on bacterial growth using diverse bacteria species that could potentially be exposed to this amino acid in the natural environment. We found that Rhizobiales were the most affected species by DL-CAN (Fig. 3A) while *P. putida* growth was not affected even at high levels of DL-CAN (up to 10 mM) (Fig. S5A) suggesting that producer species (i.e., encoding a broad-spectrum racemase) might have developed tolerance to DL-CAN.

Although DL-CAN induced PG modifications in all species tested, Rhizobiales displayed the highest levels of muro^{CAN}, i.e., ca. 40% of the muropeptides were edited by D-CAN both in the fourth and fifth positions of the peptide moieties (Fig. 3A and B, Fig. S5B).

To investigate the consequences of D-CAN incorporation on the PG architecture, we added increasing concentrations of DL-CAN to *A. tumefaciens* and monitored fluctuation of the different PG components. Our results show that DL-CAN causes a dramatic increase in pentapeptides (M5 and D45) (Fig. 3B and C), and a reduction in crosslinkage due to lower amount of LD-crosslinked muropeptides (Fig. 3D). L-CAN alone did not change *A. tumefaciens* PG crosslinkage at tested concentration (Fig. S5C).

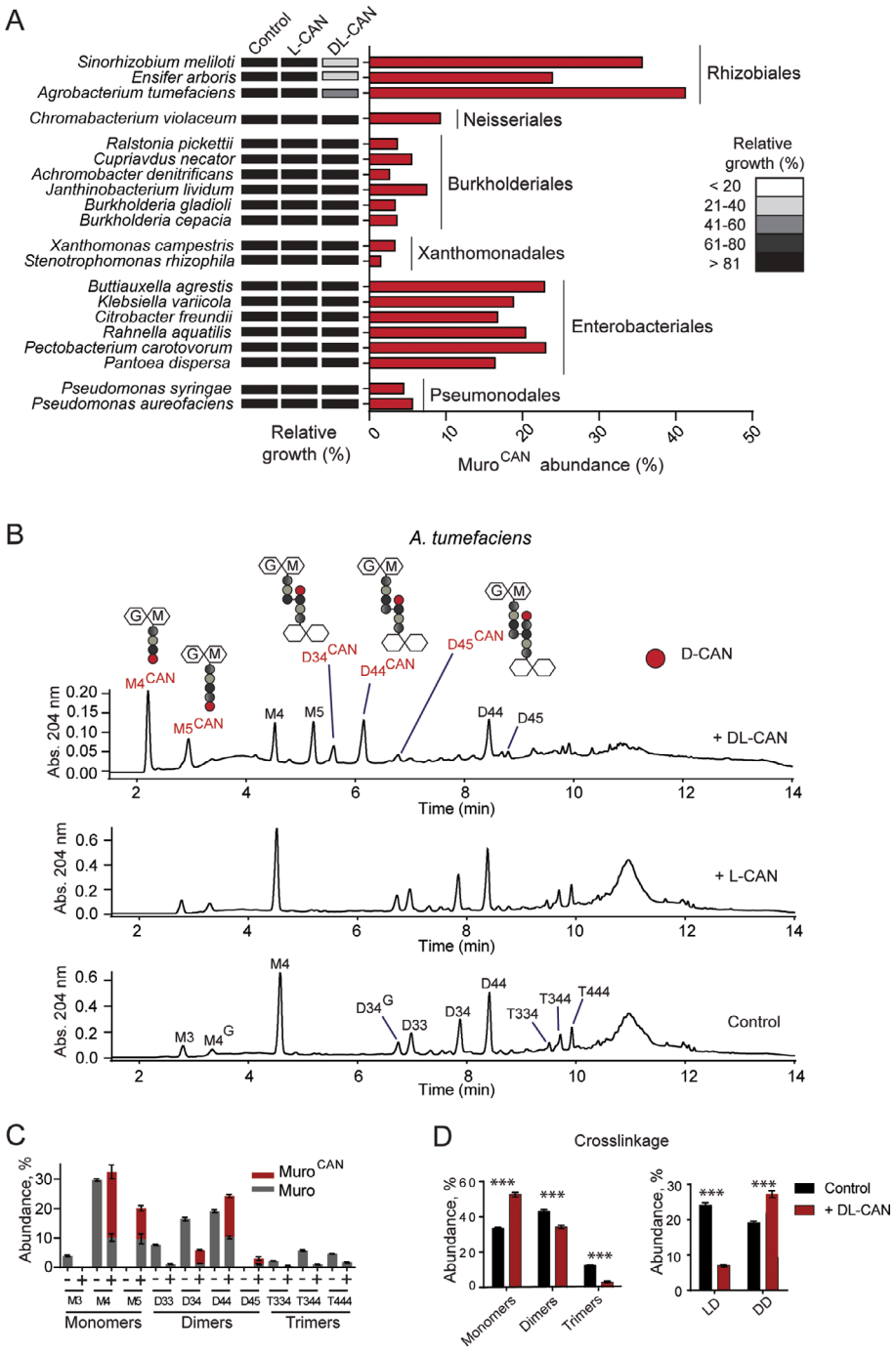

Fig 3. High D-CAN incorporation changes structure and amount of peptidoglycan in *Agrobacterium tumefaciens*.
A. Sensitivity of soil and ubiquitous bacteria to DL-CAN. Relative growth was calculated for bacteria grown without CAN, in the presence of 2.5 mM L-CAN or 5 mM DL-CAN. D-CAN incorporation was measured for bacteria supplemented with 2.5 mM DL-CAN.
B. Representative PG profiles of *A. tumefaciens* supplemented with DL-CAN 10 mM, L-CAN 5 mM or without CAN supplementation (control). Illustrations show D-CAN-containing muropeptides.
C. Abundance of D-CAN-containing muropeptides in *A. tumefaciens* supplemented with 10 mM DL-CAN. Monomer $M4^G$ and dimer $D34^G$ are calculated as part of non-modified M4 and D34.
D. Abundance of monomers, dimers and trimers in *A. tumefaciens* supplemented with 10 mM DL-CAN. Abundance of LD- and DD-crosslinked muropeptides in *A. tumefaciens* supplemented with 10 mM DL-CAN. *P* value <0.0001 (***).

To know if the effects of DL-CAN in *A. tumefaciens*' PG extend to other Rhizobiales, we analysed PG composition in the legume symbiont *Sinorhizobium meliloti*. As in *A. tumefaciens*, we found the same types of D-CAN modified muropeptides and increased levels of monomers in *S. meliloti* treated with DL-CAN (Figs. S5D and S5E). Interestingly, we had to use lower concentration of the compound, since *S. meliloti* was more sensitive to DL-CAN than *A. tumefaciens*. Collectively, our data demonstrates that DL-CAN can alter cell wall composition of certain Rhizobiales and affect their growth.

DL-CAN impairs viability and cell separation

To gain further insights on DL-CAN's mechanism of action, we cultured *A. tumefaciens* with or without L- or DL-CAN and monitored growth and morphology. Our

results showed that DL-CAN inhibited growth of *A. tumefaciens* in liquid culture and induced lysis, branching and bulging (Fig. 4A). No significant changes in growth or morphology were caused by L-CAN (Fig. 4A) further strengthening the idea that these enantiomers have different functions. To get more quantitative insights of the morphological defects caused by DL-CAN, we measured cell length, longitudinal position of the constriction (Fig. 4B) and the number of constrictions per cell (Fig. 4C). While in the untreated culture, or in cultures treated with L-CAN, *A. tumefaciens* division sites localized slightly closer to the new pole (Fig. 4B and Fig. S6A), in DL-CAN treated cultures cells were up to 1.5 times longer and the position of the constrictions exhibited a more scattered pattern (Fig. 4B). In addition, untreated cells and cells treated with L-CAN had 0 or 1 constriction per cell, while DL-CAN induced up to five constrictions per cell (Fig. 4C and Fig. S6A) further supporting that DL-CAN interferes with the cell division.

As before, *S. meliloti* grown on DL-CAN recapitulated the results obtained with *A. tumefaciens* on growth and morphology (Fig. S6B, C and D).

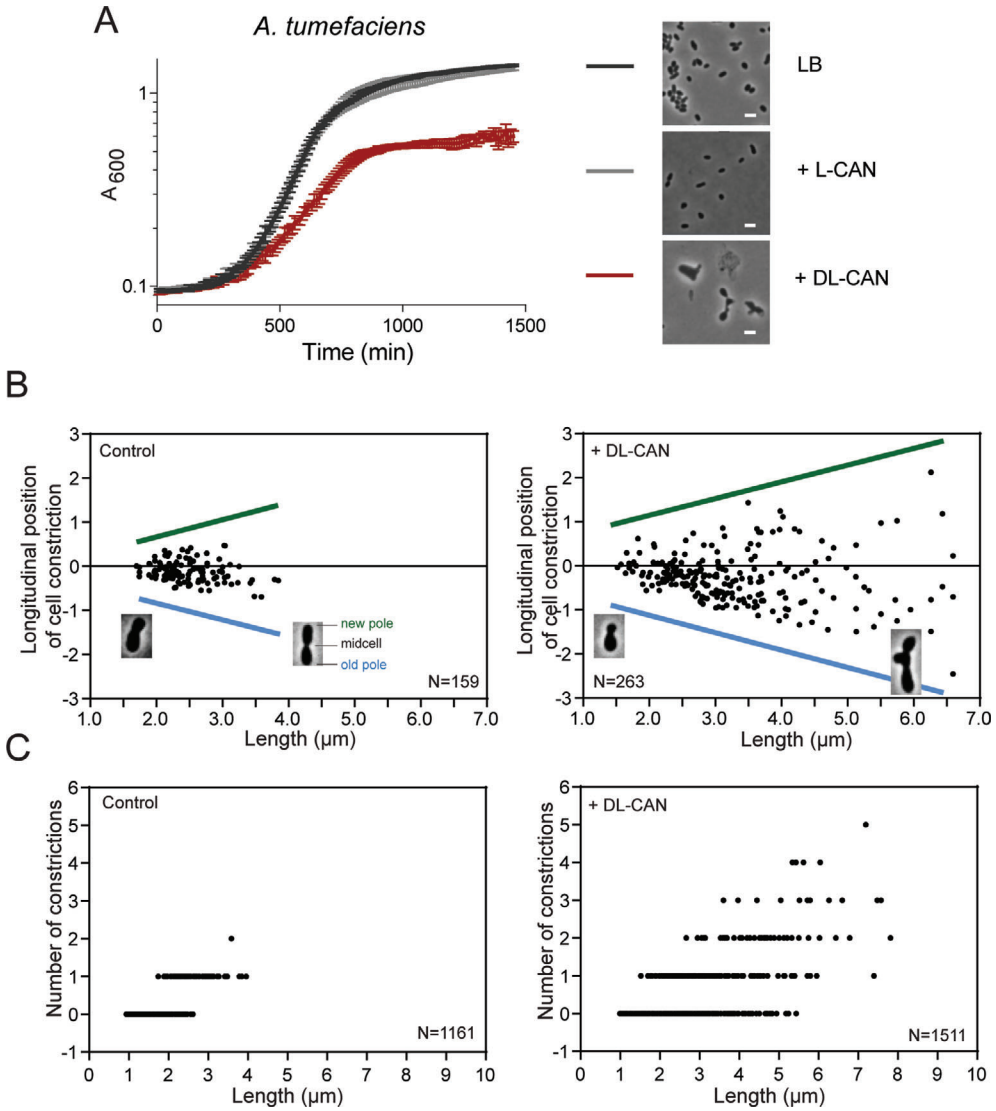

Fig 4. DL-CAN inhibits growth of *Agrobacterium tumefaciens* and leads to aberrant cell morphology.
A. Growth curves of *A. tumefaciens* in the absence (control) or presence of L-CAN 5 mM or DL-CAN 10 mM, and phase contrast images of *A. tumefaciens* cells without (control) or supplemented with L-CAN 5 mM or DL-CAN 10 mM. Scale bar 2 μm.
B. Longitudinal position of cell constriction in *A. tumefaciens* cells without (control) or with DL-CAN 10 mM. New pole is marked by green colour, old pole – by blue.
C. Number of constrictions per cell in *A. tumefaciens* grown without (control) or with DL-CAN 10 mM.

Single amino acid substitution in the cell division PG transpeptidase PBP3a partially suppresses DL-CAN detrimental effect

To identify the molecular targets of DL-CAN, we screened for suppressor mutants. Characterization of the single-nucleotide polymorphism by genome sequencing revealed a K537R substitution in the primary cell division transpeptidase PBP3a (*atu2100*; Cameron *et al*., 2014; Figueroa-Cuilan and Brown, 2018). Phyre2 alignments (Kelley *et al*., 2015) of *A. tumefaciens* PBP3a to crystallized PBP3 proteins localized K537 in the loop between β5 and λ11, close to the active-site cleft (Fig. 5A).

Reconstruction of the K537R mutation (i.e., *A. tumefaciens* PBP3a^{K537R}) by allelic exchange to confirm the role of this single-nucleotide polymorphism recapitulated the suppressor tolerance to DL-CAN (Fig. 5B). Interestingly, K537R substitution appeared to be specific since it did not suppress the growth inhibitory effect of D-AAs other than D-Arg, a chemical analogue of D-CAN (Fig. S7). No difference in the growth of the wt and PBP3a^{K537R} strains was detected in the absence or presence of L-CAN (Fig. S8A).

Both wild-type vs. the PBP3a^{K537R} strains showed similar levels of D-CAN containing muropeptides (muro^{CAN}) in cultures supplemented with DL-CAN indicating that the suppressing role of the PBP3a^{K537R} mutations is not associated with a reduction of D-CAN incorporation in the PG (Fig. S8B).

Consistent with a potential negative effect of DL-CAN on PBP3a activity, the PBP3a^{K537R} strain showed a reduction in the accumulation of pentapeptides (i.e., M5) compared to that of the wild-type in the presence of DL-CAN (Fig. 5C and Fig. S8C). Overall crosslinkage levels and particularly LD-crosslinkage also improved in the PBP3a^{K537R} strain (Fig. 5D and Fig. S8D), while no difference between strains was observed in control condition (Fig. S8E). Similarly, altered cell length and constriction positioning in the presence of DL-CAN improved in the PBP3a^{K537R} strain compared to wt (Fig. 5E), while no difference was observed in the control condition or in the presence of L-CAN (Fig. 5E and Fig. S8F). Collectively, these data show that a single mutation in PBP3a transpeptidase improves *A. tumefaciens* fitness in the presence of DL-CAN.

Discussion

Bacteria can edit the canonical chemistry of their cell wall as a strategy to cope with environmental challenges (Horcajo *et al*., 2012; Espaillat *et al*., 2016; Yadav *et al*., 2018). As PG can be modified by secreted molecules, we reasoned that we could use bacteria as a biochemical trap to discover elusive environmental modulators of the cell wall. To test this, we exposed plant-derived soluble extracts to the soil bacteria *P. putida* and discovered CAN as a new PG modulator. The fact that L-CAN was previously reported to be produced by legume plants (Bell, 1958; Rosenthal and Nkomo, 2000) further supported the efficacy of our screening. However, CAN was found at the terminal position of the PG peptide moieties, which is reserved for D-AAs (Lam *et al*., 2009). Remarkably, we found that *P. putida* encodes a Bsr that changes the chirality of CAN to permit its incorporation in the bacterial PG. Collectively, these observations underscore a fascinating example of interspecies metabolic crosstalk where a plant-derived metabolite (L-CAN) is transformed by a bacterial enzyme (BSAR) into a previously unrecognized molecule (D-CAN; Fig. 6). Discovery of D-CAN adds to a growing list of metabolites produced as a result of plant–soil feedbacks and contributes to chemical ecology (Planchamp *et al*., 2015; Etalo *et al*., 2018; Hu *et al*., 2018).

Since amino acid enantiomers have different functions, L- to DL-CAN racemization and diffusion of D-CAN into surroundings may lead to multiple environmental effects. On one side, BSAR racemization of L-CAN to DL-CAN decreases the concentration of the L-CAN, alleviating its toxic effect on plants (Miersch *et al*., 1992). In addition, BSAR produces D-CAN, a compound that alters bacterial PG composition (Fig. 6).

PG editing is a mechanism by which the environment can regulate the cell wall structure and biosynthesis. Whether this regulation is positive or detrimental seems to depend both on the type of D-AA and on the bacteria species. For instance, although *V. cholerae* produces and incorporates both D-Arg and D-Met in its PG, only the latter has an effect on cell wall synthesis (Alvarez *et al*., 2018). In the particular case of DL-CAN, it seems clear that the most sensitive species were those with polar growth and higher levels of D-CAN in the PG. Indeed, many Rhizobiales elongate unidirectionally by adding PG to the new pole, generated after cell division (Brown *et al*., 2012). When new cell compartment gets bigger in length and width, the zone of active PG growth together with division proteins localize to midcell prior to cell division. In *A. tumefaciens* multiple LD-transpeptidases are encoded (e.g., 14 Ldts in *A. tumefaciens* compared to just two predicted orthologues in *P. putida*) and different Ldts are localized to the new pole or midcell, and presumably important for both polar growth and division (Cameron *et al*., 2014). Ldts are the enzymes that perform mDAP-mDAP crosslinks, which are very abundant in Rhizobiales (40%–50% in *A. tumefaciens*) compared to e.g., *P. putida* (ca. 1%), and catalyse PG editing in the fourth position of the peptide moieties (Cava *et al*., 2011). Therefore, free DL-CAN

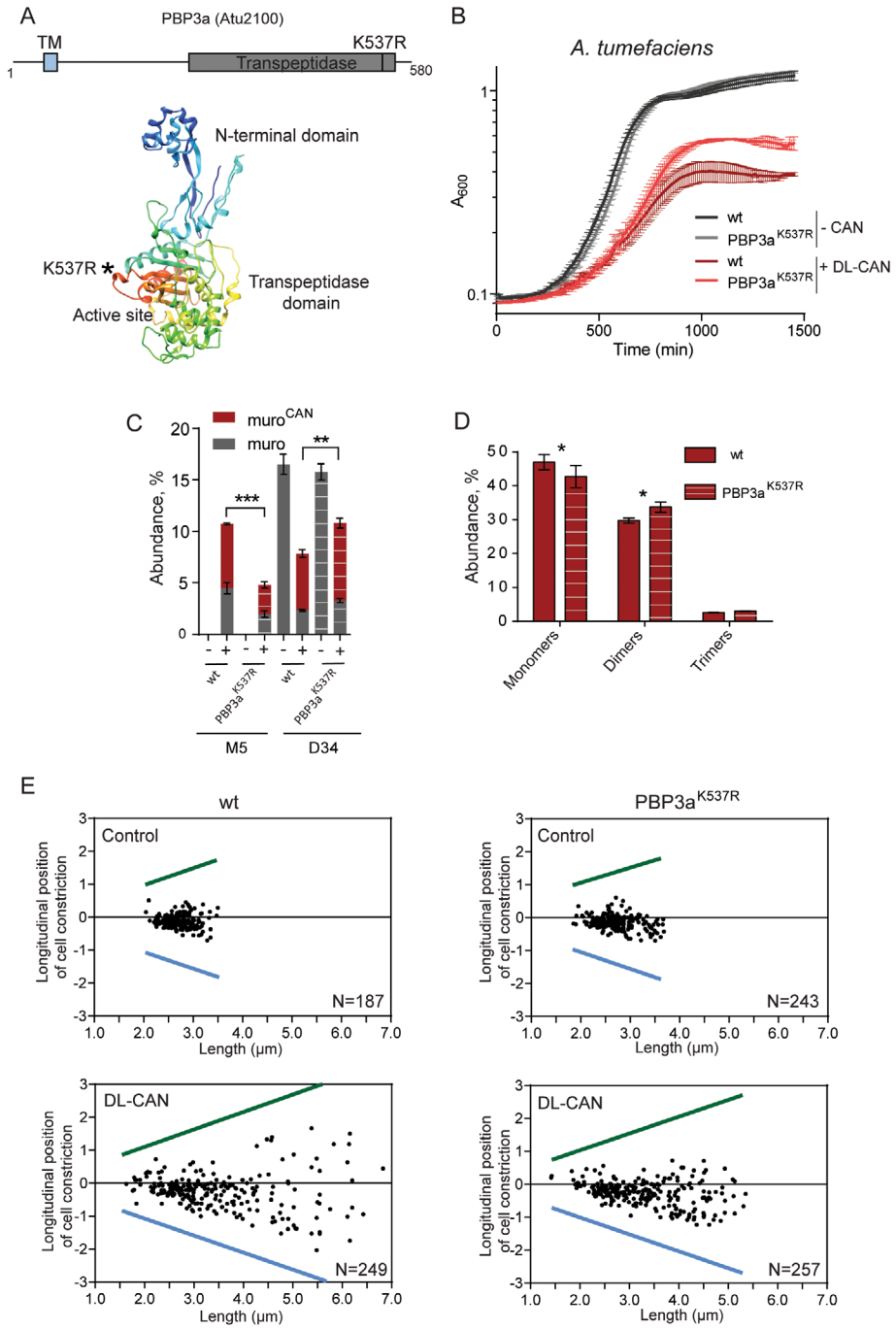

Fig 5. K537R amino acid change in *Agrobacterium tumefaciens* PBP3a protein provides resistance to DL-CAN.
A. Position of the PBP3a K537R amino acid change in the protein scheme and in the protein structural prediction based on a homology model.
B. Growth curves of *A. tumefaciens* wild type and PBP3a^{K537R} without CAN and in the presence of DL-CAN 10 mM.
C. Quantification of the monomer (M5) and dimer (D34) abundance in *A. tumefaciens* wild type and PBP3a^{K537R} grown with DL-CAN 10 mM. *P*-value <0.005 (**) and < 0.0001 (***).
D. Abundance of monomers, dimers and trimers in *A. tumefaciens* wild type and PBP3a^{K537R} supplemented with 10 mM DL-CAN. *P*-value <0.05 (*).
E. Longitudinal position of cell constriction in *A. tumefaciens* wild type and PBP3a^{K537R} cells without (control) or with DL-CAN 10 mM. New pole is marked by green colour, old pole – by blue.

might act as a competitive substrate on Ldts to prevent their LD-crosslinking activity in favour of high D-CAN incorporation. In fact, D33 and D34 LD-crosslinked dimers are significantly reduced in the presence of DL-CAN. The high number of Ldt paralogues in these species suggests they are important for the lifestyle of these organisms and thus might be difficult to assess whether a DL-CAN deleterious effect can be suppressed in a Ldt-deficient strain. Another target of DL-CAN inhibition might be DD-carboxypeptidases, enzymes that remove the terminal D-Ala from pentapeptides (M5). Accumulation of both the canonical (D-Ala-terminated pentapeptides) and the non-canonical (D-CAN-pentapeptides) in the presence of DL-CAN strongly suggest that free DL-CAN decreases the activity of *A. tumefaciens* DD-carboxypeptidases.

Interestingly, our suppressor analyses did not identify any mutations in Ldts or DD-carboxypeptidases that improved the growth of *A. tumefaciens* in the presence of

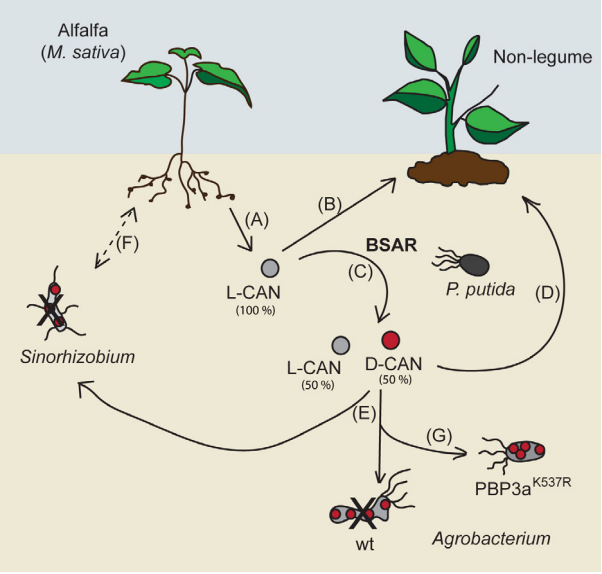

Fig 6. Model summarizing results of this work.
A. L-CAN is produced by many legumes (e.g., alfalfa, jack beans) in high amounts (Bell, 1958; Rosenthal and Nkomo, 2000).
B. L-CAN inhibits growth of plant non-producers (Rosenthal, 1970).
C. BSAR produces DL-CAN from L-CAN.
D. DL-CAN is less toxic to *Arabidopsis thaliana* than L-CAN.
E. DL-CAN severely alters cell wall composition, impairs viability and affects morphology in *Sinorhizobium meliloti* and *Agrobacterium tumefaciens*.
F. DL-CAN might negatively affect symbiotic relationship of L-CAN producer Alfalfa and its symbionts *Sinorhizobia*.
G. DL-CAN effect on *A. tumefaciens* is relieved by a K537R mutation in PBP3a. Continues lines point to information published before or presented in the current work.

DL-CAN. The high number of Ldt and DD-carboxypeptidase paralogues (14 and 4 predicted respectively) makes very unlikely that a single mutation in these proteins would show a suppressor effect. Instead, we discovered that a K537R point mutation in the PBP3a (*atu2100*) is sufficient to alleviate DL-CAN sensitivity in *A. tumefaciens*. There are two important evidences in agreement with the idea of DL-CAN targeting PBP3a: (i) PBP3a has been reported to localize at the septum and be involved in cell division. Consistently, DL-CAN induces branching and bulging in the wt and the PBP3a K537R mutation suppresses this phenotype (Fig. 6). (ii) PBP3a is a DD-transpeptidase. Inhibition of these enzymes reduce crosslinkage levels and increase accumulation of the monomeric substrates (pentapeptide and/or tetrapeptide monomers, i.e., M5 and M4 respectively). Indeed, DL-CAN induces M5 accumulation in the wt, which is suppressed in the K537R mutant. Overall DD-crosslinkage is not reduced by DL-CAN, but it is possible that DL-CAN targets PBP3a and other PBPs are not inhibited.

The nature of the observed increase in D34 dimers in the K537R mutant seems to be indirect while yet connected to the presence of DL-CAN. D34 dimers are formed between two monomer tetrapeptides (M4) by LD-transpeptidases, not by PBP3a, which is a DD-transpeptidase and would produce a D43 dimer instead. One might speculate that structural changes in the septal PBP3a might have allosteric consequences on nearby enzymes within the same protein complex. In this line, it has been reported that several Ldt enzymes predominantly localize to the midcell at cell division in *A. tumefaciens* (Cameron *et al*., 2014). Therefore, it might possible that PBP3a K537R mutation influences the activity of septal Ldts. Alternatively, PBP3a K537R mutation might induce allosteric regulatory changes in DD-carboxypeptidase at the septum, leading to local consumption of pentapeptides at cell division and increase in the levels of M4, which as Ldt substrates, can boost formation of D34. Collectively, these results suggest that D-CAN incorporation downregulates PBP3a, among other cell wall associated activities, to inhibit cell division and induce cell lysis. We hypothesize that K537R substitution might change the properties of the loop between β5 and λ11, which is proximal to the active-site cleft to preserve PBP3a activity while making it insensitive to DL-CAN. Understanding the structural changes that K-R mutation induces in the PBP3a structure might provide insights about the underlying mechanisms behind DL-CAN tolerance in other bacterial species.

Finally, we have demonstrated that DL-CAN also affects *S. meliloti* cell wall and growth. Certain legumes establish symbiosis with this bacterium for nitrogen fixation (Long, 1989). Recent studies have shown that a DD-carboxypeptidase is critical for the bacteroid (specialized nitrogen-fixing cells) differentiation in *Bradyrhizobium* spp. (Gully *et al*., 2016; Barrière *et al*., 2017). Presence of DL-CAN in *S. meliloti* milieu might disturb proper symbiosis establishment due to growth suppression or potential DD-carboxypeptidase inhibition (Fig. 6). Moreover, L-CAN was shown to inhibit *S. meliloti exp* genes expression, which are responsible for the production of symbiotically important exopolysaccharide II (Keshavan *et al*., 2005). Conversion of L- into DL-CAN by Bsr enzymes might change this gene regulation and symbiosis effectiveness.

Finally, racemization of plant amino acid L-CAN by BSAR of *P. putida* might be just one example of many where microbial broad spectrum racemases control the chirality of amino acids in the natural environment. Bsr-encoding bacteria include facultative pathogens (e.g., *V. cholerae, Proteus mirabilis* and *Xenorhabdus nematophila)*, and environmental species (e.g., *P. putida* and *Photobacterium profundum)* inhabiting diverse ecological niches (Espaillat *et al*., 2014). D-AAs diffuse in the environment and can modify the canonical chemistry of

the PG (Lam *et al*., 2009; Cava *et al*., 2011), a property that has been used to label PG biosynthesis in bacteria (Kuru *et al*., 2012; Hsu *et al*., 2016, 2017), suggesting that Bsr are drivers of cell wall chemical plasticity in the environment. However, D-AAs are also known to impact cellular processes other than cell wall biogenesis such as biofilm development, sporulation or virulence (Aliashkevich *et al*., 2018), and can often cause bacterial growth inhibition (Alvarez *et al*., 2018). Future research efforts based on multi-omic studies of complex environments that include Bsr-encoding bacteria will help to mechanistically understand the impact of D-AAs in biodiversity and physiology.

Experimental procedures

Media and growth conditions

Detailed information about strains (Table S1) and growth conditions is listed in Supplementary materials and methods. All strains were grown at the optimal temperature and in LB (Luria–Bertani broth) medium unless otherwise stated. Growth of diverse bacterial species shown in Fig. 3A was performed at room temperature.

Seed extract preparation and use of P. putida *to identify the presence of PG-modifying metabolites*

Three gram of *M. sativa* seeds were mashed and soaked in 10 ml of water overnight followed by centrifugation at 5000 rpm to remove the particulate fraction. The supernatant was next (i.e., extract) filter-sterilized and concentrated 5x. *P. putida* were grown either in LB medium or in LB medium supplemented with seed extract to a final concentration 1×. Cultures were grown up to stationary phase prior PG purification and analysis by liquid chromatography and by mass spectrometry.

Peptidoglycan analysis

PG isolation and analysis were done according previously described methods (Desmarais *et al*., 2013; Alvarez *et al*., 2016). In brief, PG sacculi were obtained by boiling bacterial cells in SDS 5%. SDS was removed by ultracentrifugation, and the insoluble material was further digested with muramidase (Cellosyl). Soluble muropeptides were separated by liquid chromatography (HPLC and/or ultra high-pressure liquid chromatography) and identified by mass spectrometry. A detailed protocol is described in Supplementary materials and methods.

Protein expression and purification

P. putida gene PP3722 encoding broad-spectrum racemase was amplified with FCP1097 (5′-AAAACATATGCCCTTTCGCCGTACC-3′) and FCP1098 (5′- AAAAGCGGCCGCGTCGACGAGTAT-3′) primers and cloned in pET22b for expression in *E. coli* Rosetta 2 (DE3) cells, resulting in C-terminal His-tagged protein.

Protein was purified using Ni-NTA agarose column (Qiagen). A detailed protocol is described in Supplementary materials and methods.

Racemase activity assay

Five microgram of purified racemase and various concentration of L-CAN in 50 μl of 50 mM sodium phosphate buffer pH 7.5 were incubated at 37°C for 30 min, then heat inactivated (5 min, 100°C), and centrifuged (15,000 rpm, 10 min). Supernatant was derivatized with Marfey's reagent (Thermo Scientific) and resolved by HPLC as described previously (Espaillat *et al*., 2014). Detailed protocols are available in Supplementary materials and methods.

BSAR *mutant construction in* P. putida

For deletion of PP3722 in *P. putida* the upstream and downstream regions of the gene were amplified from purified genomic DNA with primers FCP1145 (5′-AAAATCTAGATCATCAGCAGCGACAT-3′) and FCP1 092 (5′-CAATGGCAATTGGTGATTACTCGTGTTC-3′); FCP1093 (5′-GAGTAATCACCAATTGCCATTGAAAGGA G-3′) and FP1146 (5′-AAAATCTAGAGCGACGTCACGC-3′) respectively. The upstream and downstream fragments were combined with FCP1145 and FCP1146 into a 1010 bp fragment, and inserted into pCVD442 (Donnenberg and Kaper, 1991). *E. coli* DH5α λPIR was used in the cloning and the resulting plasmid pCVD442*BSAR* was confirmed by sequencing. In-frame deletion was introduced by allele replacement via homologous recombination. In short, exconjugants were obtained by conjugating with Sm10 λPIR containing pCVD442*BSAR* and selected on LB plates with chloramphenicol 25 μg ml^{-1} and carbenicillin 1000 μg ml^{-1}. Exconjugants were grown in LB with 10% sucrose (w/v) medium overnight and then plated on LB plates with chloramphenicol 25 μg/ml and 10% (w/v) sucrose. Colonies sensitive to carbenicillin were confirmed by PCR.

A. thaliana *growth*

A. thaliana was grown in ½ MS agar medium (half strength of Murashige and Skoog basal salt mixture (Sigma), 0.5% sucrose, 1% agar, with pH adjusted to

5.7) with or without CAN supplementation. Ethanol sterilized seeds were pre-incubated on the plates in the darkness at 4°C for 3 days before moving to the *in vitro* chamber with day/night cycle 16/8 h, 22°C/18°C. Root length was measured after 10 days of growth in the chamber with Fiji (Ducret *et al*., 2016). Pictures of the root hairs were taken with stereomicroscope Nikon SMZ1500 (Tokyo, Japan).

Growth curves and relative growth

At least three replicates per strain and growth condition were grown in 200 µl of LB alone or supplemented with CAN in a 96-well plate at 30°C with 140 rpm shaking in a BioTek Eon Microplate Spectrophotometer (BioTek, Winooski, VT, USA). The A600 was measured at 10 min intervals. Relative growth was calculated as a percentage of growth without CAN or in the presence of L- or DL-CAN compared to growth without CAN.

Phase contrast microscopy

Stationary phase bacteria were placed on 1% agarose LB pads. Phase contrast microscopy was done using a Zeiss Axio Imager.Z2 microscope (Zeiss, Oberkochen, Germany) equipped with a Plan-Apochromat 63X phase contrast objective lens and an ORCA-Flash 4.0 LT digital CMOS camera (Hamamatsu Photonics, Shizuoka, Japan), using the Zeiss Zen Blue software.

Quantification of cell constrictions

Stationary phase bacteria were placed on 1% agarose LB pads. Cell length and constrictions on phase contrast microscopy images were detected using the MicrobeJ software (Ducret *et al*., 2016). Old poles were identified as having a larger maximum width compared to the new poles. The longitudinal position of cell constrictions was then plotted against cell length. A longitudinal position of 0 represents the true midcell while positive values approach the new pole and negative values approach the old cell.

Suppressor mutants

To obtain suppressor mutants, *A. tumefaciens* was grown at optimal conditions overnight (see Supplementary methods), and serial dilutions were inoculated on the LB plates containing DL-CAN 10 mM. Plates were incubated at room temperature until suppressor mutant colonies arose. For confirmation of the resistance, the selected colonies were passed through LB plates before being tested on LB plates containing DL-CAN 10 mM.

Whole-genome sequencing and single-nucleotide polymorphism analysis

Genomic DNA was isolated from suppressor mutants and the parental strain of *A. tumefaciens*. Indexed paired-end libraries were prepared and sequenced in a MiSeq sequencer (Illumina, San Diego, CA, USA) according to the manufacturer's instructions.

Data quality control was performed with FastQC v0.11.5 (http://www.bioinformatics.babraham.ac.uk/projects/fastqc) and MultiQC v1.5 (Ewels *et al*., 2016). The raw data in FASTQ format was trimmed using Trimmomatic v0.36 with arguments 'ILLUMINACLIP: adapters.fa:2:30:10', 'SLIDINGWINDOW:5:30' and 'MINLEN:50' (Bolger *et al*., 2014). The exact adapter sequences that were used can be retrieved from the supplementary materials and methods. The trimmed FASTQ was aligned to genome GCF_000092025.1_ASM9202v1 (*A. tumefaciens*, (Wood *et al*., 2001)) using the 'mem' algorithm in BWA v0.7.15-r1140 (Li, 2013) with default parameters and subsequently converted to sorted BAM format. Optical duplicates were marked using picard tools v2.18.2 with default arguments (http://broadinstitute.github.io/picard). Finally, variants were called in freebayes v1.1.0-dirty using the parameters '-p 1', '–min-coverage 5' and '–max-coverage 500' (Erik and Gabor, 2012).

DNA sequencing data deposition

Sequencing data is deposited at The European Nucleotide Archive with primary accession numbers ERS5599687 (*Agrobacterium tumefaciens* C58 DL-CAN suppressor mutant) and ERS5599686 (*Agrobacterium tumefaciens* C58 wt).

Reconstruction of suppressor mutant pbp3a^{K537R} *in* A. tumefaciens

For reconstruction of point mutation in *pbp3a*^{K537R} in *A. tumefaciens*, a 650 bp fragment containing the mutated nucleotide was amplified from purified genomic DNA with primers FCP3354 (5′-AAAAGGATCCCGACAC CGTTGG-3′) and FCP3355 (5′- AAAAGGATCCA TAAGACACGAGCA-3′) and inserted into pNPTS139 plasmid (Fischer *et al*., 2002). *E. coli* DH5α λPIR was used in the cloning and the resulting plasmid pNPTS139*pbp3a*^{K537R} was confirmed by sequencing.

Nucleotide substitution in *A. tumefaciens pbp3a* gene (atu2100) was done according to an established allelic-replacement protocol (Morton and Fuqua, 2012a). In short, exconjugants were obtained by conjugating with *E. coli* S17-1 λPIR containing pNPTS139*pbp3a*^{K537R} and selected on ATGN plates with kanamycin 300 µg ml^{-1}.

Exconjugants were grown in ATGN medium overnight and then plated on ATSN plates with 5% (w/v) sucrose (Morton and Fuqua, 2012b). Colonies sensitive to kanamycin were streak-purified twice on ATSN plates and sequenced.

PBP3a protein folding prediction

Prediction of PBP3a protein was done by Phyre2 (Kelley *et al*., 2015).

Statistical analysis

All statistical analyses were performed using GraphPad Prism (GraphPad Software, San Diego, CA, USA). Student's unpaired *t* tests were used.

Acknowledgements

We thank Miguel Angel de Pedro and all the members of the Cava lab, particularly Laura Alvarez, Sara Hernandez and Akbar Espaillat for helpful discussions. We thank Barbara Terebienec for help with *A. thaliana* experiment.

Author contributions

Conceived and designed the experiments: A.A., M.H., P.J.B.B., and F.C. Performed the experiments: A.A., M.H. Analysed the data: A.A., M.H., P.J.B.B., and F.C. Wrote the paper: A.A., and F.C. All authors commented on the article.

Data and materials availability

All data needed to evaluate the conclusions in the article are present in the article and/or the Supplementary Materials. Additional data related to this article may be requested from the authors.

References

Aliashkevich, A., Alvarez, L., and Cava, F. (2018) New insights into the mechanisms and biological roles of D-amino acids in complex eco-systems. *Front Microbiol* **9**: 1–11.

Alvarez, L., Aliashkevich, A., de Pedro, M.A., and Cava, F. (2018) Bacterial secretion of D-arginine controls environmental microbial biodiversity. *ISME J* **12**: 438–450.

Alvarez, L., Hernandez, S.B., de Pedro, M.A., and Cava, F. (2016) Ultra-sensitive, high-resolution liquid chromatography methods for the high-throughput quantitative analysis of bacterial cell wall chemistry and structure. *Methods Mol Biol* **1440**: 11–27.

Bakker, M.G., Schlatter, D.C., Otto-Hanson, L., and Kinkel, L.L. (2014) Diffuse symbioses: roles of plant-plant, plant-microbe and microbe-microbe interactions in structuring the soil microbiome. *Mol Ecol* **23**: 1571–1583.

Barrière, Q., Guefrachi, I., Gully, D., Lamouche, F., Pierre, O., Fardoux, J., *et al*. (2017) Integrated roles of BclA and DD-carboxypeptidase 1 in Bradyrhizobium differentiation within NCR-producing and NCR-lacking root nodules. *Sci Rep* **7**: 1–13.

Bell, E.A. (1958) Canavanine and related compounds in Leguminosae. *Biochem J* **70**: 617–619.

Berendsen, R.L., Vismans, G., Yu, K., Song, Y., de Jonge, R., Burgman, W.P., *et al*. (2018) Disease-induced assemblage of a plant-beneficial bacterial consortium. *ISME J* **12**: 1496–1507.

Bolger, A.M., Lohse, M., and Usadel, B. (2014) Trimmomatic: a flexible trimmer for Illumina sequence data. *Bioinformatics* **30**: 2114–2120.

Brown, P.J.B., De Pedro, M.A., Kysela, D.T., Van Der Henst, C., Kim, J., De Bolle, X., *et al*. (2012) Polar growth in the alphaproteobacterial order Rhizobiales. *PNAS* **109**: 1697–1701.

Cameron, T.A., Anderson-Furgeson, J., Zupan, J.R., Zik, J. J., and Zambryski, P.C. (2014) Peptidoglycan synthesis machinery in *Agrobacterium tumefaciens* during unipolar growth and cell division. *MBio* **5**: 1–10.

Cava, F., de Pedro, M.A., Lam, H., Davis, B.M., and Waldor, M.K. (2011) Distinct pathways for modification of the bacterial cell wall by non-canonical D-amino acids. *EMBO J* **30**: 3442–3453.

Dahlman, D.L., and Rosenthal, G.A. (1975) Non-protein aminoacid-insect interactions—I. Growth effects and symptomology of L-canavanine consumption by tobacco hornworm, *Manduca sexta* (L.). *Comp Biochem Physiol A Comp Physiol* **51**: 33–36.

Dahlman, D.L., and Rosenthal, G.A. (1976) Further studies of the effect of L-canavanine on the tobacco hornworm, Manduca sexta. *J Insect Physiol* **22**: 265–271.

Desmarais, S.M., De Pedro, M.A., Cava, F., and Huang, K. C. (2013) Peptidoglycan at its peaks: how chromatographic analyses can reveal bacterial cell wall structure and assembly. *Mol Microbiol* **89**: 1–13.

Djordjevic, M.A., Redmond, J.W., Batley, M., and Rolfe, B.G. (1987) Clovers secrete specific phenolic compounds which either stimulate or repress nod gene expression in *Rhizobium trifolii*. *EMBO J* **6**: 1173–1179.

Doebeli, M., and Knowlton, N. (1998) The evolution of interspecific mutualisms. *Proc Natl Acad Sci U S A* **95**: 8676–8680.

Donnenberg, M.S., and Kaper, J.B. (1991) Construction of an eae deletion mutant of enteropathogenic *Escherichia coli* by using a positive-selection suicide vector. *Infect Immun* **59**: 4310–4317.

Ducret, A., Quardokus, E.M., and Brun, Y.V. (2016) MicrobeJ, a tool for high throughput bacterial cell detection and quantitative analysis. *Nat Microbiol* **1**: 16077.

Duran, P., Thiergart, T., Garrido-Oter, R., Agler, M., Kemen, E., Schulze-Lefert, P., and Hacquard, S. (2018) Microbial Interkingdom interactions in roots promote Arabidopsis survival. *Cell* **175**: 973–983.e14.

Erik, G. and Gabor, M. (2012) Haplotype-based variant detection from short-read sequencing. *arXiv Prepr arXiv12073907*.

Espaillat, A., Carrasco-López, C., Bernardo-García, N., Pietrosemoli, N., Otero, L.H., Álvarez, L., *et al*. (2014)

Structural basis for the broad specificity of a new family of amino-acid racemases. *Acta Crystallogr D Biol Crystallogr* **70**: 79–90.

Espaillat, A., Forsmo, O., El Biari, K., Björk, R., Lemaitre, B., Trygg, J., *et al*. (2016) Chemometric analysis of bacterial peptidoglycan reveals atypical modifications that empower the cell wall against predatory enzymes and fly innate immunity. *J Am Chem Soc* **138**: 9193–9204.

Etalo, D.W., Jeon, J.-S., and Raaijmakers, J.M. (2018) Modulation of plant chemistry by beneficial root microbiota. *Nat Prod Rep* **35**: 398–409.

Ewels, P., Magnusson, M., Lundin, S., and Käller, M. (2016) MultiQC: summarize analysis results for multiple tools and samples in a single report. *Bioinformatics* **32**: 3047–3048.

Figueroa-Cuilan, W.M., and Brown, P.J.B. (2018) Cell Wall biogenesis during elongation and division in the plant pathogen *Agrobacterium tumefaciens*. *Curr Top Microbiol Immunol* **418**: 87–110.

Fischer, B., Rummel, G., Aldridge, P., and Jenal, U. (2002) The FtsH protease is involved in development, stress response and heat shock control in *Caulobacter crescentus*. *Mol Microbiol* **44**: 461–478.

Gully, D., Gargani, D., Bonaldi, K., Grangeteau, C., Chaintreuil, C., Fardoux, J., *et al*. (2016) A peptidoglycan-remodeling enzyme is critical for bacteroid differentiation in *Bradyrhizobium* spp. during legume symbiosis. *Mol Plant Microbe Interact* **29**: 447–457.

Hernandez, S.B., Dorr, T., Waldor, M.K., and Cava, F. (2020) Modulation of peptidoglycan synthesis by recycled cell wall tetrapeptides. *Cell Rep* **31**: 107578.

Hibbing, M.E., Fuqua, C., Parsek, M.R., and Peterson, S.B. (2010) Bacterial competition: surviving and thriving in the microbial jungle. *Nat Rev Microbiol* **8**: 15–25.

Hills, G.M. (1949) Chemical factors in the germination of spore-bearing aerobes; the effects of amino acids on the germination of *Bacillus anthracis*, with some observations on the relation of optical form to biological activity. *Biochem J* **45**: 363–370.

Horcajo, P., De Pedro, M.A., and Cava, F. (2012) Peptidoglycan plasticity in bacteria: stress-induced peptidoglycan editing by noncanonical D-amino acids. *Microb Drug Resist* **18**: 306–313.

Hsu, Y.P., Meng, X., and VanNieuwenhze, M.S. (2016) Methods for visualization of peptidoglycan biosynthesis. *Methods Microbiol* **43**: 3–48.

Hsu, Y.-P., Rittichier, J., Kuru, E., Yablonowski, J., Pasciak, E., Tekkam, S., *et al*. (2017) Full color palette of fluorescent d-amino acids for in situ labeling of bacterial cell walls. *Chem Sci* **8**: 6313–6321.

Hu, L., Robert, C.A.M., Cadot, S., Zhang, X., Ye, M., Li, B., *et al*. (2018) Root exudate metabolites drive plant-soil feedbacks on growth and defense by shaping the rhizosphere microbiota. *Nat Commun* **9**: 1–13.

Keller, L., and Surette, M.G. (2006) Communication in bacteria: an ecological and evolutionary perspective. *Nat Rev Microbiol* **4**: 249–258.

Kelley, L.A., Mezulis, S., Yates, C.M., Wass, M.N., and Sternberg, M.J.E. (2015) The Phyre2 web portal for protein modeling, prediction and analysis. *Nat Protoc* **10**: 845–858.

Keshavan, N.D., Chowdhary, P.K., Donovan, C., and González, J.E. (2005) L-Canavanine made by *Medicago sativa* interferes with quorum sensing in *Sinorhizobium meliloti* L-Canavanine made by *Medicago sativa* interferes with quorum sensing in *Sinorhizobium meliloti*. *J Bacteriol* **187**: 8427–8436.

Kim, D.-R., Cho, G., Jeon, C.-W., Weller, D.M., Thomashow, L.S., Paulitz, T.C., and Kwak, Y.-S. (2019) A mutualistic interaction between streptomyces bacteria, strawberry plants and pollinating bees. *Nat Commun* **10**: 4802.

Kuru, E., Hughes, H.V., Brown, P.J., Hall, E., Tekkam, S., Cava, F., *et al*. (2012) In situ probing of newly synthesized peptidoglycan in live bacteria with fluorescent D-amino acids. *Angew Chem Int Ed Engl* **51**: 12519–12523.

Kuru, E., Radkov, A., Meng, X., Egan, A., Alvarez, L., Dowson, A., *et al*. (2019) Mechanisms of incorporation for D-amino acid probes that target peptidoglycan biosynthesis. *ACS Chem Biol* **14**: 2745–2756.

Lam, H., Oh, D.-C., Cava, F., Takacs, C.N., Clardy, J., de Pedro, M.A., and Waldor, M.K. (2009) D-amino acids govern stationary phase cell wall remodeling in bacteria. *Science* (80-) **325**: 1552–1555.

Li, H. (2013) Aligning sequence reads, clone sequences and assembly contigs with BWA-MEM. *arXiv:13033997v2*.

Long, S.R. (1989) Rhizobium-legume nodulation: life together in the underground. *Cell* **56**: 203–214.

Mandel, M.J., Wollenberg, M.S., Stabb, E.V., Visick, K.L., and Ruby, E.G. (2009) A single regulatory gene is sufficient to alter bacterial host range. *Nature* **458**: 215–218.

Miersch, J., Jühlke, C., Sternkopf, G., and Krauss, G.J. (1992) Metabolism and exudation of canavanine during development of alfalfa (*Medicago sativa* L. cv. verko). *J Chem Ecol* **18**: 2117–2129.

Molina, L., Ramos, C., Duque, E., Ronchel, M.C., Wyke, L., and Ramos, J.L. (2000) Survival of *Pseudomonas putida* KT2440 in soil and in the rhizosphere of plants under greenhouse and environmental conditions. **32**: 315–321.

Morton, E.R., and Fuqua, C. (2012). Genetic manipulation of agrobacterium. *Current Protocols in Microbiology*, **25**. http://dx.doi.org/10.1002/9780471729259.mc03d02s25.

Morton, E.R., and Fuqua, C. (2012b) Laboratory maintenance of Agrobacterium. *Curr Protoc Microbiol* **Chapter 1**: Unit3D.1. **24**.

Pines, M., Rosenthal, G.A., and Applebaum, S.W. (1982) In vitro incorporation of L-canavanine into vitellogenin of the fat body of the migratory locust Locusta migratoria migratorioides. *Proc Natl Acad Sci U S A* **78**: 5480–5483.

Planchamp, C., Glauser, G., and Mauch-mani, B. (2015) Root inoculation with *Pseudomonas putida* KT2440 induces transcriptional and metabolic changes and systemic resistance in maize plants. **5**: 1–10.

Poliakov, A., Russell, C.W., Ponnala, L., Hoops, H.J., Sun, Q., Douglas, A.E., and Van Wijk, K.J. (2011) Large-scale label-free quantitative proteomics of the pea aphid-Buchnera Symbiosis. *Mol Cell Proteomics* **10**: M110.007039.

Radkov, A.D., and Moe, L.A. (2013) Amino acid racemization in *Pseudomonas putida* KT2440. *J Bacteriol* **195**: 5016–5024.

Radkov, A.D., and Moe, L.A. (2018) A broad spectrum racemase in *Pseudomonas putida* KT2440 plays a key role in amino acid catabolism. *Front Microbiol* **9**: 1343.

Rosenthal, A.G., and Nkomo, P. (2000) The natural abundance of L-canavanine, an active anticancer agent, in Alfalfa, *Medicago sativa* (L.). *Pharm Biol* **38**: 1–6.

Rosenthal, G.A. (1970) Investigations of Canavanine biochemistry in the Jack Bean, *Canavalia ensiformis* (L.) DC. *Plant Physiol* **46**: 273–276.

Rosenthal, G.A. (1977) Nitrogen allocation for L-Canavanine synthesis and its relationship to chemical defense of the seed. *Biochem Syst Ecol* **5**: 219–220.

Rosenthal, G.A., and Dahlman, D.L. (1991) Studies of L-canavanine incorporation into insectan lysozyme. *J Biol Chem* **266**: 15684–15687.

Rosenthal, G.A., Lambert, J., and Hoffmann, D. (1989) Canavanine incorporation into the antibacterial proteins of the fly, *Phormia terranovae* (Diptera), and its effect on biological activity. *J Biol Chem* **264**: 9768–9771.

Scott, J.J., Oh, D.C., Yuceer, M.C., Klepzig, K.D., Clardy, J., and Currie, C.R. (2008) Bacterial protection of beetle-fungus mutualism. *Science (80-)* **322**: 63.

Shaw, L.J., Morris, P., and Hooker, J.E. (2006) Perception and modification of plant flavonoid signals by rhizosphere microorganisms. *Environ Microbiol* **8**: 1867–1880.

Weller, D.M. (1988) Biological control of soilborne plant pathogens in the rhizosphere with bacteria. *Annu Rev Phytopathol* **26**: 379–407.

Wood, D.W., Setubal, J.C., Kaul, R., Monks, D.E., Kitajima, J.P., Okura, V.K., *et al*. (2001) The genome of the natural genetic engineer *Agrobacterium tumefaciens* C58. *Science* **294**: 2317–2323.

Yadav, A.K., Espaillat, A., and Cava, F. (2018) Bacterial strategies to preserve cell wall integrity against environmental threats. *Front Microbiol* **9**: 1–9.

Supporting Information

Additional Supporting Information may be found in the online version of this article at the publisher's web-site:

Fig. S1 PG profiles and mass analyses of *P. putida* grown without (control) and with the alfalfa seed extract. N-deAc: N-deacetylated muropeptide; Lys: Lysine; Arg: Arginine; N: anhydromuropeptides.

Fig. S2 (A) Mass spectra of the PG of *P. putida* grown without or with the alfalfa seed extract at the retention time were the new muropeptide (peak 3) was detected (ca. 1.9 min). The indicated molecular ion corresponds to the double charged form of the new muropeptide. (B) MS fragmentation pattern of the peak 3 in the PG of *P. putida* grown with the alfalfa seed extract. (C) Theoretical and experimental molecular masses of $M4^{CAN}$ and $D44^{CAN}$ detected in the PG of *P. putida* grown with 5 mM L-CAN. (D) MS fragmentation pattern of $M4^{CAN}$ detected in the PG of *P. putida* grown with 5 mM L-CAN. (E) PG profiles of *P. putida* grown with the alfalfa seed extract spiked with increasing amount of purified $M4^{CAN}$. (F) MS fragmentation pattern of $D44^{CAN}$ detected in the PG of *P. putida* grown with 5 mM L-CAN.

Fig. S3 (A) Muropeptide profile of the PG of *P. putida* grown without and with the alfalfa seed extract obtained by LC using separation methods 1 and 2. (B) PG analysis of *P. putida* wild-type and Δ*BSAR* grown with the addition of 5 mM of L-CAN. Note that LC separation method 2 was used. (C) D-amino acids quantification in supernatants of *P. putida* wt and Δ*BSAR* grown without or with 10 mM L-Ala, L-Leu, L-Ser, L-Met, L-Arg or L-CAN. (D) PG analysis of *E. coli* grown in PCM of *P. putida* wild-type and Δ*BSAR*, which was cultured without L-CAN or with 5 mM L-CAN. Note that LC separation method 2 was used.

Fig. S4 (A) Root length in *A. thaliana* grown on ½ Murashige-Skoog agar supplemented with L-CAN 5 and 10 μM, and DL-CAN 10 and 20 μM. (B) Representative pictures of root system in *A. thaliana* grown on ½ Murashige-Skoog agar supplemented with L- or DL-CAN 20 μM or not (control).

Fig. S5 (A) Growth curves of *P. putida* in LB in the absence (0 mM) or presence of L- or DL-CAN. (B) Masses and structure of CAN-modified muropeptides. (C) Abundance of monomers, dimers and trimers in *A. tumefaciens*, grown in LB medium (control) or LB medium supplemented with L-CAN 5 mM. (D) Representative PG profiles of *S. meliloti* grown without (control) or with L-CAN 1.5 mM or DL-CAN 3 mM. (E) Abundance of monomers, dimers and trimers in *S. meliloti*, grown in LB medium (control) or LB medium supplemented with L-CAN 1.5 mM or DL-CAN 3 mM. P value <0.005 (**).

Fig. S6 (A) Longitudinal position of cell constriction and number of constrictions in *A. tumefaciens* cells with L-CAN 5 mM. (B) Growth curves of *S. meliloti* in LB medium without CAN or supplemented with L-CAN 1.5 mM or DL-CAN 3 mM. (C) Phase contrast images of *S. meliloti* cells without (control) or supplemented with L-CAN 1.5 mM or DL-CAN 3 mM. Scale bar 2 μm. (D) Longitudinal position of cell constriction in *S. meliloti* cells with L-CAN 1.5 mM or DL-CAN 3 mM or without addition of CAN (control).

Fig. S7 Growth curves of *A. tumefaciens* wild-type and $PBP3a^{K537R}$ without and with supplementation of different D-amino acids.

Fig. S8 (A) Growth curves of *A. tumefaciens* wild-type and $PBP3a^{K537R}$ in LB medium or in LB medium supplemented by L-CAN 5 mM. (B) Abundance of D-CAN-containing muropeptides in *A. tumefaciens* wild-type and $PBP3a^{K537R}$ grown with or without DL-CAN 10 mM. P-value <0.005 (**) and < 0.0001 (***). (C) Abundance of LD- and DD-crosslinked muropeptides in *A. tumefaciens* wild-type and $PBP3a^{K537R}$ supplemented with 10 mM DL-CAN. (D) Abundance of monomers, dimers and trimers and LD- and DD-crosslinked muropeptides in *A. tumefaciens* wild-type and $PBP3a^{K537R}$, grown in LB medium (control). (E) Abundance of total amount of D-CAN-containing muropeptides in *A. tumefaciens* wild-type and $PBP3a^{K537R}$ supplemented with 10 mM DL-CAN. (F) Longitudinal position of cell constriction in *A. tumefaciens* wild-type and $PBP3a^{K537R}$ cells with L-CAN 5 mM.

Appendix S1: Supporting Information